



Ignition of hydrogen/air mixtures by a heated kernel: Role of Soret diffusion

Wenkai Liang^{a,*}, Chung K. Law^{a,b}, Zheng Chen^c

^a Department of Mechanical and Aerospace Engineering, Princeton University, Princeton, NJ 08544, USA

^b Center for Combustion Energy, Tsinghua University, Beijing 100084, China

^c Department of Mechanics and Aerospace Engineering, Peking University, Beijing 100871, China



ARTICLE INFO

Article history:

Received 18 May 2018

Revised 26 June 2018

Accepted 22 August 2018

Keywords:

Minimum ignition energy

Soret diffusion

Hydrogen

ABSTRACT

Effects of Soret diffusion on the ignition of hydrogen/air mixtures by a heated kernel, and the structure and dynamics of the embryonic flame that is subsequently formed, were investigated numerically with detailed chemistry and transport. Results show that Soret diffusion leads to larger (smaller) *minimum ignition energy* (MIE) for relatively rich (lean) mixtures, that this effect is mainly engendered by the Soret diffusion of H₂ while that of the H radical is almost negligible, and that Soret diffusion also leads to an increase (decrease) of the Markstein length for rich (lean) mixtures. Satisfactory agreement with literature experimental data on the MIE is shown, especially for the critical states near lean and rich flammability limits. Evolution of the flame structure shows that before the self-sustained flame is formed, the high temperature gradient associated with the ignition kernel has driven the H₂ in the mixture towards the ignition kernel and formed a locally high H₂ concentration region, which consequently renders lean (rich) mixtures easier (harder) to ignite. It is further shown that Soret diffusion of both H and H₂ affect the *propagation dynamics* of the stretched spherical flame that is subsequently formed, from its embryonic state until that of free propagation, in that Soret diffusion of H₂ is the dominant mode at small flame radius with the large strain rate, while that of H is the dominant mode at large flame radius with the small strain rate similar to that of the unstretched adiabatic planar flame.

© 2018 The Combustion Institute. Published by Elsevier Inc. All rights reserved.

1. Introduction

Ignition of a flammable mixture by a localized thermal deposition is of extensive practical interest, ranging from spark ignition within internal combustion engines to the accidental initiation of fires and explosions. Mechanistically, a successful ignition event would require both the formation of an embryonic flame before the ignition kernel is diffusively dissipated, and the attainment of this embryonic flame to achieve free propagation independent of the imposed state of the ignition kernel. Since steep temperature gradients result from the application of the localized high-temperature ignition kernel, Soret diffusion [1,2], which drives light species towards the high temperature region and heavy species away from it, could exert notable influence on the failure or success of ignition. Furthermore, it is also well established that successful ignition depends on the amount of energy deposited, which is characterized by the minimum ignition energy (MIE) [2,3] and has been extensively studied numerically [4,5] and

experimentally [3,6]. It is clear that Soret diffusion, whose influence depends on the steepness of the temperature gradient, could substantially affect the MIE.

In terms of prior contributions on Soret diffusion in combustion problems, we note the studies on metal particles [7], soot [8–10], and *n*-heptane [11] for the heavy fuel species, and those on the light fuel species of hydrogen, methane, and syngas by Ern and Giovangigli [12,13], Bongers and De Goey [14], Grcar et al. [15], Yang et al. [16,17], Liang et al. [18] and Faghii et al. [19] with specific interests on the flame propagation velocities and stretch-induced extinction limits. The problem has also been theoretically analyzed by Han and Chen [20]. Mechanistically, in these studies the temperature gradients driving Soret diffusion arise from existing flames, while large concentration gradients are also already present such that Fickian diffusion is expected to be dominant, with Soret diffusion having only secondary effects. For the present ignition problem, however, the initial species concentrations are uniform and the imposed heat deposition generates a local high-temperature region before chemical reactions can substantially alter the concentration profiles. Consequently, Soret diffusion could impose substantial and mechanistically quite different influences.

* Corresponding author.

E-mail address: wenkail@princeton.edu (W. Liang).

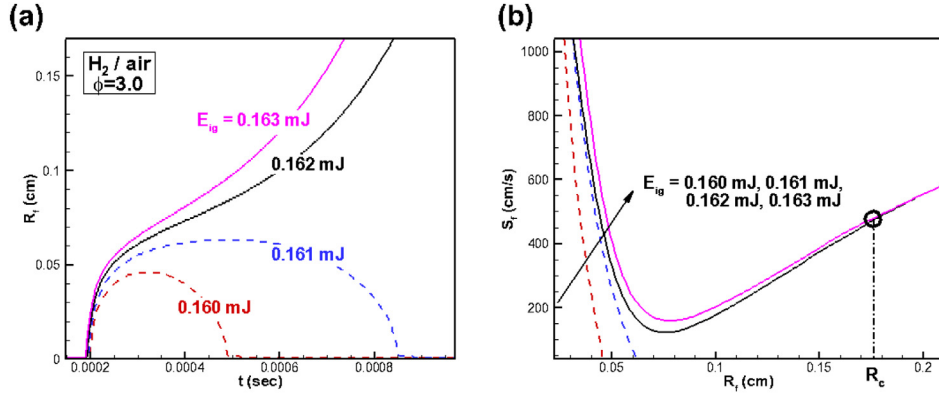


Fig. 1. Spherical flame initiation for hydrogen/air mixtures ($\phi=3.0$) at different ignition energies: (a) temporal variation of flame radius; (b) flame propagation speed as a function of flame radius.

The objective of the present study is to study the effects of Soret diffusion on ignition of hydrogen/air mixtures by a heated kernel, and quantitatively assess and explain its influence on the MIE. Specifically, the unsteady, spherically symmetric flame is first simulated to calculate the MIE of hydrogen/air mixtures to demonstrate the flame initiation and propagation processes. Next, the physical model and computational method used in this study are briefly described. Then, results on MIE and the related length scale – namely the Markstein length, are discussed and the flame front evolution with detailed flame structure is presented. Finally concluding remarks are given.

2. Numerical method and problem specification

The problem of interest was studied computationally, using the A-SURF code [21] which solves the conservation equations of 1-D, compressible, reactive flow in a spherical coordinate, and has been successfully used and validated in previous studies [21–23]. A multi-level, dynamically adaptive mesh is used and the moving reaction zone is always fully covered by the fine meshes. The thermodynamic and transport properties as well as the reaction rates were calculated using the CHEMKIN packages [24], using the detailed hydrogen/air reaction mechanism of Li et al. [25]. The mixture-averaged formulation [1] has been adopted to calculate both the Fickian and Soret diffusion fluxes, and the results compared with those using more detailed multicomponent formulation were found to be close.

The mixture is initially homogeneous, at 298 K and atmospheric pressure. Imposition of the ignition kernel is given by:

$$q_{iq} = \begin{cases} \frac{E_{ig}}{\pi^3/2 r_{ig}^3 t_{ig}} \exp\left[-\left(\frac{r}{r_{ig}}\right)^2\right] & \text{if } t < t_{ig} \\ 0 & \text{if } t \geq t_{ig} \end{cases} \quad (1)$$

where E_{ig} is the total ignition energy, t_{ig} the duration of the energy source, and r_{ig} the ignition kernel radius. The ignition kernel size and duration for most cases are fixed as $t_{ig}=200 \mu\text{s}$ and $r_{ig}=200 \mu\text{m}$, respectively. Figure 1(a) shows the time evolution of the flame radius for different ignition energies with $\phi=3.0$. It is seen that a self-sustained propagating flame can only be successfully initiated when the ignition energy is above the MIE. The MIE can be determined by the average of the ignition energies for the closest success and failure cases of ignition, which gives $E_{min}=0.1615 \text{ mJ}$ for this mixture. The MIE for all other mixtures were determined similarly, with an uncertainty below 5%. In addition to the MIE, studies [26,27] have shown that there also exists a critical flame radius, R_c , beyond which flame propagates as a

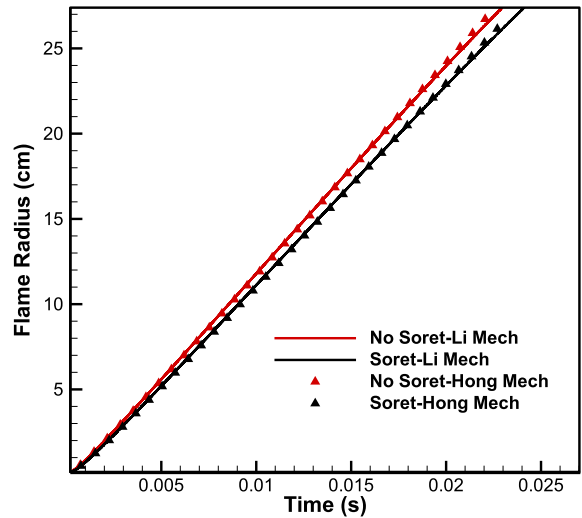


Fig. 2. Spherical flame initiation for hydrogen/air mixtures ($\phi=3.0$) with different kinetic mechanisms ($E_{ig}=0.5 \text{ mJ}$).

self-sustained quasi-steady flame independent of the ignition energy. This gives a characteristic dimension of the ignition and flame propagation process. Based on this criterion, the critical radius was defined as the point where the ignition energy does not affect the subsequent flame propagation; specifically $R_c=0.176 \text{ cm}$, as indicated by the circle symbol in Fig. 1(b).

Furthermore, to validate the chosen kinetic mechanism, the flame trajectories using an updated hydrogen mechanism by Hong et al. [28] are compared in Fig. 2. It is found that given the same ignition energy, differences due to the kinetic mechanism are quantitatively small and qualitatively do not lead to any change in the understanding of the effect of Soret diffusion.

3. Results and discussion

3.1. MIE and related length scales

Figure 3(a) shows the calculated MIE for mixtures with equivalence ratio ϕ ranging up to 5.2. Since the possible candidate species for substantial Soret diffusion in hydrogen flames are H_2 , the fuel, and H, the intermediate radical, we focus on their separate roles on the MIE. In Fig. 3(a), it is seen that Soret diffusion significantly affects MIE for extremely lean and rich cases, at which the MIE increases rapidly as the mixture is close to the flammability limits. Furthermore, the effect of Soret diffusion has opposite

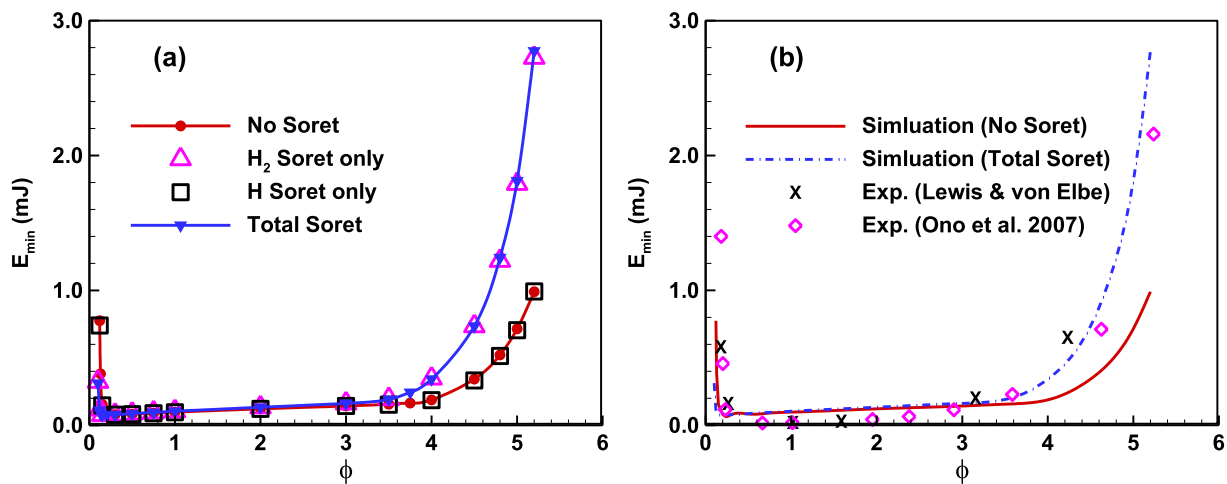


Fig. 3. MIE of hydrogen/air mixtures (a) simulation results allowing Soret diffusion for different species; (b) comparison with experimental data in Refs. [3,6].

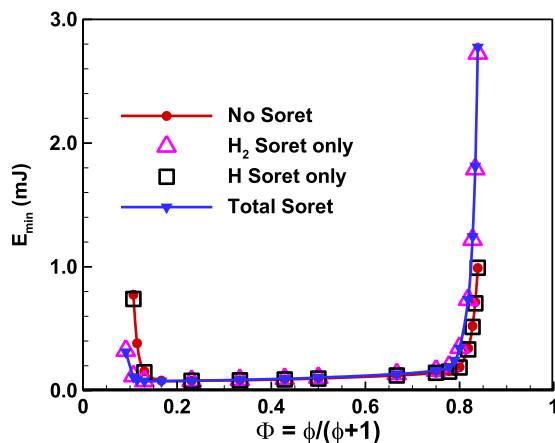


Fig. 4. MIE of hydrogen/air mixtures versus normalized equivalence ratio.

influence on the MIE near the lean/rich flammability limits, which would decrease/increase the MIE. Regarding the dominant species for the Soret effect, the fuel, H_2 , is found to determine the MIE, which has almost identical effect compared with the cases considering Soret diffusions of all species; while the influence of the radical, H, Soret diffusion only asserts minimal influence on the MIE. This finding is very different from previous results on the laminar flame speeds affected by Soret diffusion [16] and the reasons will be given in the following subsections.

To validate the simulation, its results are compared with the experimental data from Refs. [3,6] in Fig. 3(b). It is noted that the MIE at rich and lean limit cases are well captured by the simulation with total Soret diffusion. However, simulated MIE values without Soret diffusion near the rich flammability limit show considerable shift.

In Fig. 3, we see that variation of MIE at the lean side is much steeper than that at the rich side. However, by implementing the more appropriate definition of the normalized equivalence ratio [2], $\Phi = \phi/(\phi + 1)$, where ϕ is the conventionally defined equivalence ratio, we see that a plot of MIE versus Φ (Fig. 4) yields a profile that is considerably more symmetrical as compared to Fig. 3. Consequently, the gentler slope for MIE on the rich side in Fig. 3, as compared to the steeper slope on the lean side, is largely a consequence of the asymmetrical definition of ϕ , and has no bearing on the physical nature of lean-versus-rich preference.

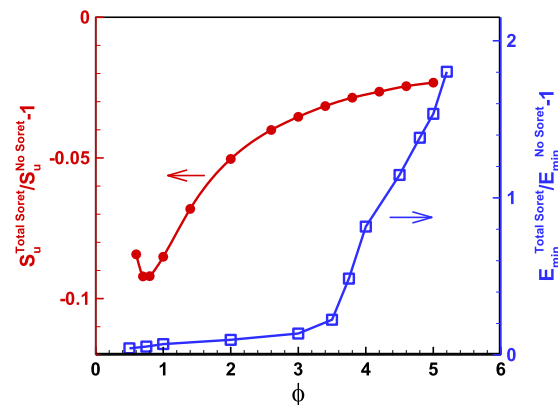


Fig. 5. Relative changes in the laminar flame speed and minimum ignition energy caused by the inclusion of Soret diffusion of all species.

To assess the relative changes caused by the inclusion of Soret diffusion, the relative difference in MIE due to Soret diffusion is presented in Fig. 5. As comparison, the relative changes in the laminar flame speed calculated by the PREMIX code [29] are also plotted in Fig. 5. It is found that near the rich flammability limit, Soret effect can lead to errors in MIE as large as 100% to 200%. This is to be contrasted with results on the laminar flame speed of hydrogen/air mixtures, showing that Soret diffusion reduces the laminar flame speed and only has a minimally discernible influence. Such finding indicates that it is necessary to include the Soret diffusion for accurate predictions of MIE.

We next note that in the classical thermal-diffusion theory, the minimum radius of the developing flame kernel for successful flame initiation is related to either the quenching distance or the flame thickness [2], both of which do not consider the specifics of flame propagation including effects of preferential diffusion. The burned Markstein length, L_b , is obtained from linear regression of the flame propagating speed, $S_b = dR_f/dt$, and the flame stretch rate, $K = (2/R_f)(dR_f/dt)$ [2,32]. Figure 6 shows that L_b increases with ϕ . This is reasonable as it is well known that L_b increases with Le [32, 33], while the effective Le increases as ϕ increases for hydrogen/air mixtures. Figure 5(a) further shows that only considering H_2 Soret diffusion leads to nearly the same extent of reduction in L_b as that by allowing Soret diffusion of all species, and that the L_b without Soret diffusion of all species is close to that of including only H Soret diffusion. These results therefore demonstrate that only change of L_b is mainly caused by the Soret diffusion

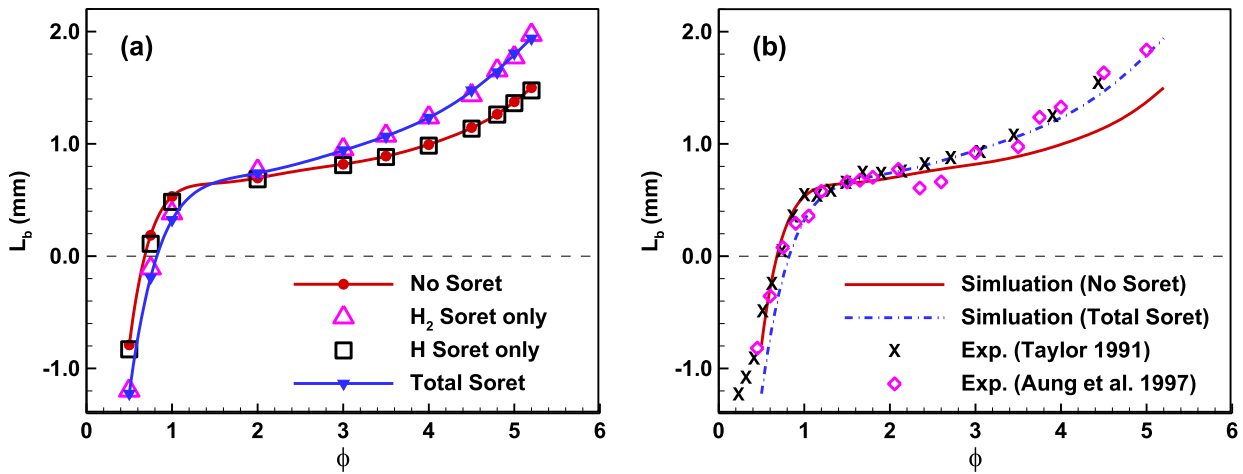


Fig. 6. Burned Markstein length of hydrogen/air mixtures (a) allowing Soret diffusion for different species and (b) comparing with experimental data [30,31].

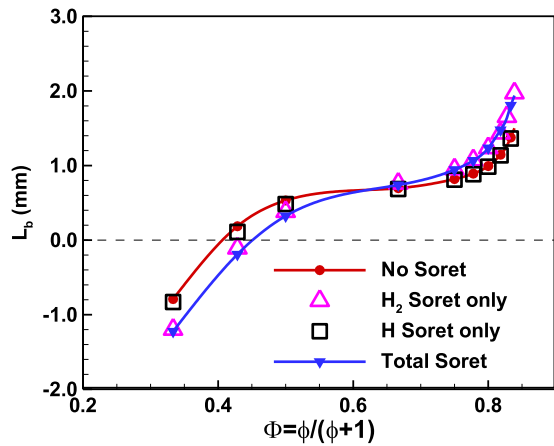


Fig. 7. Burned Markstein length of hydrogen/air mixtures versus normalized equivalence ratio.

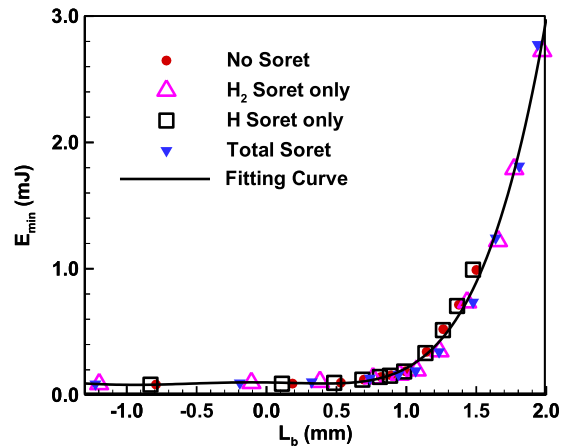


Fig. 8. Scaling of MIE with burned Markstein length allowing Soret diffusion for different species.

of H₂ rather than that of the H radical, which can be explained by two factors. First, Soret diffusion promotes the mass diffusion of H₂ and thereby effectively increases the mass diffusivity of H₂. As a result, the *Le* of H₂ is reduced when Soret diffusion of H₂ is activated. Since *L_b* decreases monotonically with decreasing *Le*, *L_b* tends to be reduced. The second factor is the change of the flame temperature due to the change of local stoichiometry. As the Soret diffusion of H₂ drives the fuel into the ignition kernel, ϕ is increased locally. For lean (rich) mixtures, the flame temperature will be increased (decreased). Thus, it leads to a smaller (larger) *L_b*. For lean mixtures, both of these two factors reduce the *L_b*. For rich mixtures, since the effective *Le* is based on the deficit species - O₂, thermal effect is the dominant one. Consequently, Fig. 5(a) shows that *L_b* increases with Soret diffusion. On the other hand, since the Soret diffusion flux of H is much less than that of H₂, the influence of Soret diffusion on the preferential diffusion between heat and H radical in a stretched flame is negligible. Consequently, depending on the value of *L_b*, the flame propagation can be either promoted, for *L_b* < 0, or inhibited, for *L_b* > 0, by the positive stretch rate. As a result, the MIE depends strongly on *L_b* - the larger the *L_b*, the larger the MIE for positive Markstein lengths. Also, Fig. 6(b) shows good agreements of the simulation results compared with the experimental data [30,31]. Similarly, using the concept of normalized equivalence ratio as just discussed, the plot of *L_b* versus Φ yields a profile that is considerably more (anti-)symmetrical, as shown Fig. 7.

Motivated by the fact that MIE has similar behavior regarding the effect of Soret diffusion on the length scale *L_b*, the scaling of MIE with *L_b* is demonstrated in Fig. 8, showing that the MIE of all the four different cases can be collapsed on a single curve, which indicates that the influence of Soret diffusion is mainly through the modification of the related length scale, namely the Markstein length.

3.2. Flame front evolution

To further understand the effects of Soret diffusion on the MIE, we investigate the flame front evolution at the state of near-limit ignition. Figs. 9 and 10 show the changes of the flame propagation speed, *S_b*, with the flame radius, *R*, and with the strain rate, *K*, for both rich ($\phi = 4.5$) and lean ($\phi = 0.5$) mixtures initially at normal temperature and pressure. For an outwardly propagating spherical flame, the strain rate is $K = 2S_b/R$ [2] and thus it is inversely proportional to the flame radius.

It is seen that, for the rich case (*Le* > 1) in Fig. 9, there are three stages of ignition: propagation of spark-assisted ignition kernel with decreasing flame speed; unsteady transition from spark ignition to normal flame propagation, represented by the transition from the minimum speed to a normal flame; and normal flame propagation following the rapid increase of the flame speed in the second stage. However, for the lean case (*Le* < 1) in Fig. 9, only two stages of ignition are identified: propagation of spark assisted igni-

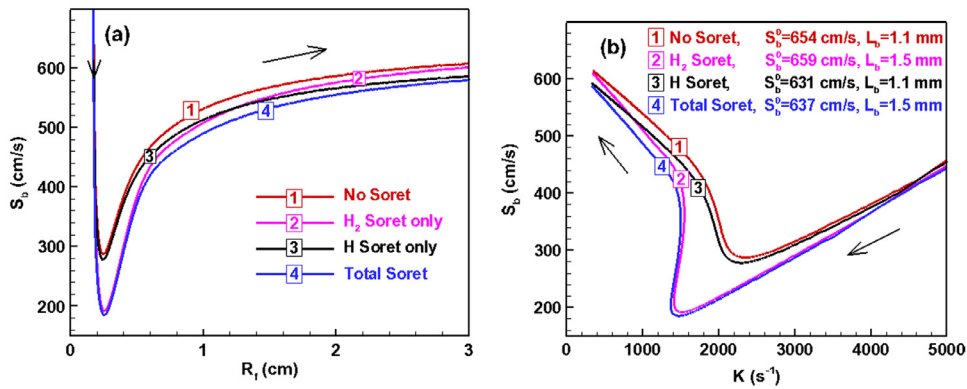


Fig. 9. Change of the spherical flame propagation speed with: (a) flame radius and (b) strain rate for rich hydrogen/air mixture at $\phi = 4.5$.

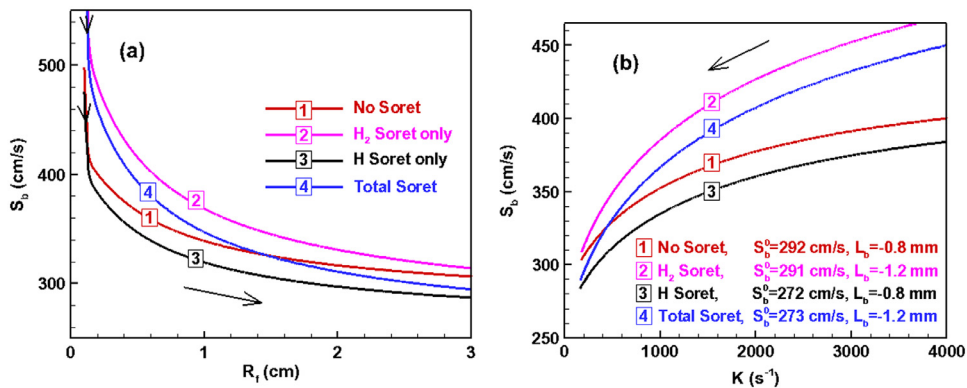


Fig. 10. Change of the spherical flame propagation speed with the (a) flame radius and (b) strain rate for lean hydrogen/air mixture at $\phi = 0.5$.

tion kernel and normal flame propagation. After the flame enters the normal flame propagation stage, it is independent of the ignition energy and the flame speed S_b varies almost linearly with the strain rate K . It is seen that the first spark-assisted ignition stage is strongly affected by Soret diffusion.

We next separately analyze the effects of Soret diffusion at large and small flame radii. At large flame radius, stretch effect on the flame propagation speed is small, as shown in Figs. 9(b) and 10(b), and thus the influence of Soret diffusion is similar to that on the unstretched planar flame. Figs. 9(a) and 10(a) indicate that the inclusion of Soret diffusion of all species reduces the flame propagation speed. Moreover, this reduction is mainly caused by the Soret diffusion of the H radical. When only the Soret diffusion of H_2 is considered, the flame speed at large radius is seen to be nearly the same as that without Soret diffusion. Consequently, Soret diffusion of H_2 (H radical) has weak (strong) influence on the flame speed at small stretch rate. These results are consistent with those on unstretched laminar flame speed discussed previously [16]. For flame propagation at small radius, Figs. 9 and 10 show that the flame propagation speed is strongly affected by the Soret diffusion of both H_2 and H and Soret diffusion of H_2 is the dominant mode. This is reasonable because preferential and second-order diffusion effects are accentuated by stretch, which has larger values at small flame radius. Consequently, Soret diffusion is expected to be inherently important for ignition because of the large stretch rate experienced by the embryonic flame.

3.3. Detailed flame structure

To further explain the role of Soret diffusion on the ignition process, we need to investigate the Fickian and Soret diffusion fluxes of H_2 and the H radical. Since previous subsections knew

that the effective species is H_2 , the focus thereafter is on the role of H_2 Soret diffusion at different stages of the ignition process. For demonstration, the rich ($\phi = 4.5$) and lean ($\phi = 0.5$) conditions are used.

Figure 11 shows the Fickian and Soret diffusion fluxes of H_2 at different times. At $t = 0.01$ ms, it is seen that the ignition kernel is still strongly influenced by the heat deposit. Specifically, if Soret diffusion of all species is considered, the Fickian diffusion flux is positive and its magnitude is almost of the same order as that of the (negative) Soret diffusion flux. Since the localized hot kernel at the early stage of ignition generates a small high temperature region, the light species, H_2 , is driven by Soret diffusion into the center of the ignition kernel and the corresponding Fickian diffusion needs to balance with this Soret diffusion to move H_2 towards the ambience. However, if Soret diffusion is not included, the Fickian diffusion flux, which is also the total diffusion flux in this case, is almost zero at the spark-assisted ignition stage. The consequence of neglecting Soret diffusion here is that for the subsequent self-sustained propagating flame, the flame kernel size is different from the case with total Soret diffusion. As shown in Fig. 11, at $t = 3$ ms, Soret diffusion would decelerate the flame for the rich case and accelerate the flame for the lean case.

To further demonstrate this phenomenon, the mole fractions of H_2 at different times with and without Soret diffusion for rich and lean mixtures are shown in Figs. 12(a) and 12(b) respectively. It is seen that if Soret diffusion is included, at $t = 0.01$ ms, there is a local region of high H_2 concentration at the center of the ignition kernel. The reason for its formation is the negative Soret diffusion fluxes shown in Fig. 11, which is activated by the imposed heat input. Then, this local high concentration will trigger Fickian diffusion towards the ambience. It is noted that such an unsteady effect is important for the initial stage of the flame formation and propa-

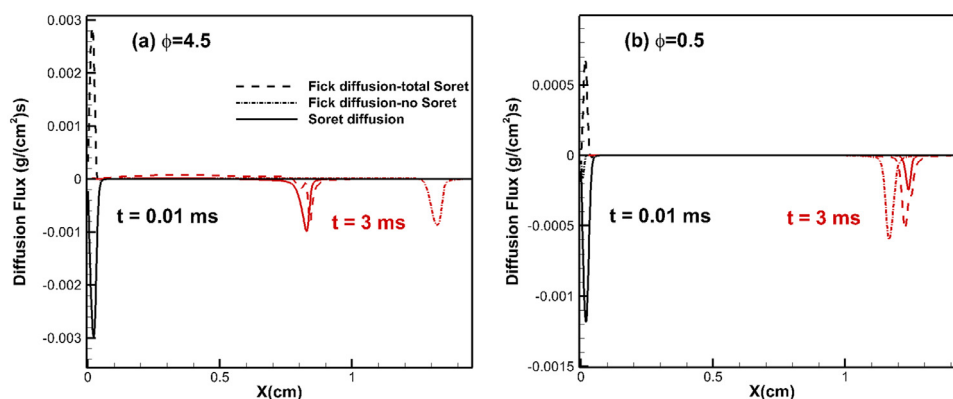


Fig. 11. Diffusion fluxes of H_2 for (a) rich ($\phi = 4.5$) and (b) lean ($\phi = 0.5$) hydrogen/air mixtures.

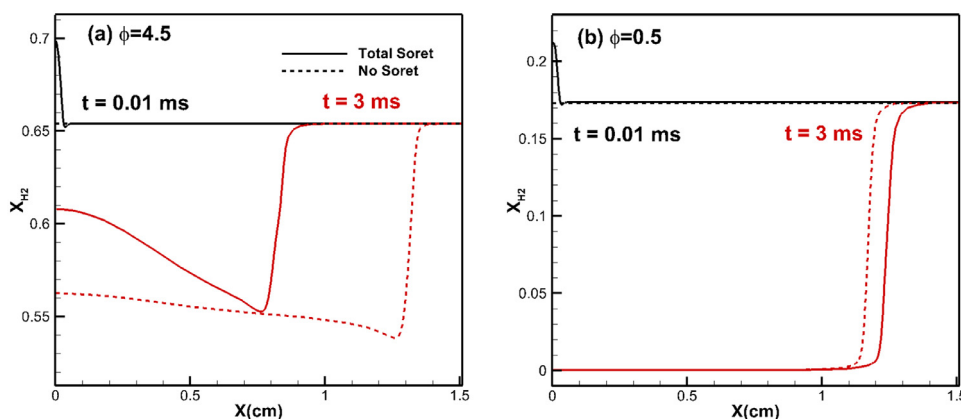


Fig. 12. Mole fractions of H_2 for (a) rich ($\phi = 4.5$) and (b) lean ($\phi = 0.5$) hydrogen/air mixtures.

gation. Also, this effect is not incorporated in the classical spherical flame theory based on quasi-steady state flame propagations.

4. Conclusions

In the present study, effects of Soret diffusion on the MIE of hydrogen/air mixtures at normal temperature and pressure are studied numerically. Results indicate that the influence of Soret diffusion increases (decreases) the MIE for relatively rich (lean) mixtures. Furthermore, it is found that this effect is mainly caused by the Soret diffusion of H_2 rather than the H radical. The related length scale, the Markstein length, was assessed with Soret diffusion of different species. It is found that Soret diffusion would increase the length scales for the rich mixtures and reduce them for the lean mixtures. Its effect on the lean side is partly due to the Lewis number since the effective Lewis number is primarily that of the deficit species, namely H_2 , whose diffusivity is strongly modified by Soret diffusion. On the rich side, the influence is largely due to the change of the local stoichiometry and hence the change of the local temperature. It is also found that Soret diffusion during the spark assisted flame propagation stage would potentially enhance the concentration of H_2 in the ignition kernel and further change the subsequent flame propagation speed.

Acknowledgments

The work at Princeton University was supported by the US National Science Foundation (CBET, Grant # 1510142) under the technical monitoring of Dr. Song-Chang Kong, while that at Peking University by the National Natural Science Foundation of China (Nos. 91741126 and 91541204). WL was in addition supported by a

Guggenheim Fellowship and a Harari Fellowship of Princeton University.

References

- [1] J.O. Hirschfelder, C.F. Curtiss, R.B. Bird, *Molecular theory of gases and liquids*, John Wiley, 1954.
- [2] C.K. Law, *Combustion physics*, Cambridge University Press, 2006.
- [3] B. Lewis, G. Von Elbe, *Combustion, flames and explosions of gases*, Academic press, New York, 1961.
- [4] Frendi, M. Sibulkin, Dependence of minimum ignition energy on ignition parameters, *Combust. Sci. Technol.* 73 (1990) 395–413.
- [5] Z. Chen, M.P. Burke, Y. Ju, On the critical flame radius and minimum ignition energy for spherical flame initiation, *Proc. Combust. Inst.* 33 (2011) 1219–1226.
- [6] R. Ono, M. Nifuku, S. Fujiwara, S. Horiguchi, T. Oda, Minimum ignition energy of hydrogen–air mixture: Effects of humidity and spark duration, *J. Electrostat* 65 (2007) 87–93.
- [7] C.J. Sung, J.S. Kistler, M. Nishioka, C.K. Law, Further studies on effects of thermophoresis on seeding particles in LDV measurements of strained flames, *Combust. Flame* 105 (1996) 189–201.
- [8] M. Arias-Zugasti, D.E. Rosner, Soret transport, unequal diffusivity, and dilution effects on laminar diffusion flame temperatures and positions, *Combust. Flame* 153 (2008) 33–44.
- [9] C.P. Leusden, C. Hasse, N. Peters, Aggregate formation in sooting counterflow diffusion flames, *Proc. Combust. Inst.* 29 (2002) 2383–2390.
- [10] S.B. Dworkin, M.D. Smooke, V. Giovangigli, The impact of detailed multicomponent transport and thermal diffusion effects on soot formation in ethylene/air flames, *Proc. Combust. Inst.* 32 (2009) 1165–1172.
- [11] Y. Xin, C.J. Sung, C.K. Law, A mechanistic evaluation of Soret diffusion in heptane/air flames, *Combust. Flame* 159 (2012) 2345–2351.
- [12] A. Ern, V. Giovangigli, Thermal diffusion effects in hydrogen-air and methane-air flames, *Combust. Theor. Model.* 2 (1998) 349–372.
- [13] A. Ern, V. Giovangigli, Impact of detailed multicomponent transport on planar and counterflow hydrogen/air and methane/air flames, *Combust. Sci. Technol.* 149 (1999) 157–181.
- [14] H. Bongers, L.P.H. De Goeij, The effect of simplified transport modeling on the burning velocity of laminar premixed flames, *Combust. Sci. Technol.* 175 (2003) 1915–1928.

- [15] J.F. Grcar, J.B. Bell, M.S. Day, The Soret effect in naturally propagating, premixed, lean, hydrogen–air flames, *Proc. Combust. Inst.* 32 (2009) 1173–1180.
- [16] F. Yang, C.K. Law, C.J. Sung, H.Q. Zhang, A mechanistic study of Soret diffusion in hydrogen–air flames, *Combust. Flame* 157 (2010) 192–200.
- [17] F. Yang, H.Q. Zhang, & X.L. Wang, Effects of Soret diffusion on the laminar flame speed of n-butane–air mixtures, *Proc. Combust. Inst.* 33(2011) 947–953.
- [18] W. Liang, Z. Chen, F. Yang, H. Zhang, Effects of Soret diffusion on the laminar flame speed and Markstein length of syngas/air mixtures, *Proc. Combust. Inst.* 34 (2013) 695–702.
- [19] M. Faghhi, W. Han, Z. Chen, Effects of Soret diffusion on premixed flame propagation under engine-relevant conditions, *Combust. Flame* 194 (2018) 175–179.
- [20] W. Han, Z. Chen, Effects of Soret diffusion on spherical flame initiation and propagation, *Int. J. Heat Mass Transfer* 82 (2015) 309–315.
- [21] Z. Chen, Effects of radiation and compression on propagating spherical flames of methane/air mixtures near the lean flammability limit, *Combust. Flame* 157 (2010) 2267–2276.
- [22] W. Zhang, Z. Chen, W. Kong, Effects of diluents on the ignition of premixed H₂/air mixtures, *Combust. Flame* 159 (2012) 151–160.
- [23] P. Dai, Z. Chen, Supersonic reaction front propagation initiated by a hot spot in n-heptane/air mixture with multistage ignition, *Combust. Flame* 162 (2015) 4183–4193.
- [24] R.J. Kee, F.M. Rupley & J.A. Miller, Report SAND89-8009B, Sandia National Laboratory (1989).
- [25] J. Li, Z. Zhao, A. Kazakov, F.L. Dryer, An updated comprehensive kinetic model of hydrogen combustion, *Int. J. Chem. Kinet.* 36 (2004) 566–575.
- [26] A.P. Kelley, G. Jomaas, C.K. Law, Critical radius for sustained propagation of spark-ignited spherical flames, *Combust. Flame* 156 (2009) 1006–1013.
- [27] H.H. Kim, S.H. Won, J. Santner, Z. Chen, Y. Ju, Measurements of the critical initiation radius and unsteady propagation of n-decane/air premixed flames, *Proc. Combust. Inst.* 34 (2013) 929–936.
- [28] Z. Hong, D.F. Davidson, R.K. Hanson, An improved H₂/O₂ mechanism based on recent shock tube/laser absorption measurements, *Combust. Flame* 158 (2011) 633–644.
- [29] R.J. Kee, J.F. Grcar, M.D. Smooke, J.A. Miller, E. Meeks. Sandia National Laboratories Report. 1985 (SAND85-8249).
- [30] S.C. Taylor, Burning velocity and the influence of flame stretch, Doctoral dissertation, University of Leeds, 1991.
- [31] K.T. Aung, M.I. Hassan, G.M. Faeth, Flame stretch interactions of laminar premixed hydrogen/air flames at normal temperature and pressure, *Combust. Flame* 109 (1997) 1–24.
- [32] G.H. Markstein, *Nonsteady flame propagation*, Pergamon, 1964.
- [33] J.K. Bechtold, M. Matalon, The dependence of the Markstein length on stoichiometry, *Combust. Flame* 127 (2001) 1906–1913.